Evolutionary Multi-objective Optimization and Decision Making for Selective Laser Sintering

Nikhil Padhye
Department of Mechanical Engineering
Indian Institute of Technology Kanpur
Kanpur-208016, India
npdhye@gmail.com

Kalyanmoy Deb
Department of Mechanical Engineering
Indian Institute of Technology Kanpur
Kanpur-208016, India
deb@iitk.ac.in

ABSTRACT

This paper proposes an integrated approach to arrive at optimal build orientations, simultaneously minimizing surface roughness 'Ra' and build time 'T', for object manufacturing in SLS process. The optimization task is carried out by two popularly known multi-objective evolutionary optimizers - NSGA-II (non-dominated sorting genetic algorithm) and MOPSO (multi-objective particle swarm optimizer). The performance comparison of these two optimizers along with an approximation of Pareto-optimal front is done using two statistically significant performance measures. Three proposals addressing the task of decision making, i.e. selecting one solution in presence of multiple trade-off solutions, are introduced to facilitate the designer. The overall procedure is integrated into $MORPE$ - Multi-objective Rapid Prototyping Engine. Several sample objects are considered for experimentation to demonstrate the working of $MORPE$. A careful study of optimal build directions for several components indicates a trend, providing insight into the SLS processes which can be regarded highly useful for various practical RP applications.

Keywords

Multi-objective Optimization, Decision Making, Genetic Algorithms, Particle Swarm Optimization and SLS.

1. INTRODUCTION

Rapid prototyping (RP) or layered manufacturing refers to processes in which a component is fabricated by layer-by-layer deposition of material from 3D computer assisted design models. RP is playing an important role in reducing the time required for new product development and lowering the development costs. Common examples of RP techniques are Fused Deposition Method (FDM), Stereolithography (SLA), Selective Laser Sintering (SLS), Laminated Object Manufacturing (LOM), 3D printing and Direct Metal Deposition (DMD). With the advent of these technologies, it is now possible to fabricate physical prototypes directly from CAD models for checking the feasibility of design concept and prototype verification.

SLS is one such popular RP process for object manufacturing [7]. Rapid growth of SLS can be attributed to its ability to process various materials like polymers, metals, ceramics and composites. Commercial SLS systems build the parts by selective solidification of the thermoplastic polymer powder by CO_2 laser. First, tessellated CAD model (represented using triangular meshes) is 'sliced', with layer thickness ranging from 0.1 to 0.3 mm. The powder is spread on the machine bed with the help of a re-coater and pre-heated to about $4-5^\circ$ C below its melting point. This is done by four heat radiators present in the built chamber. The laser is then focussed on heated powder to sinter it and cause local solidification of the material. In the sintering process the temperature of the powder is raised to a point of fusing without actual melting. After allowing sufficient time for the sintered layer to cool down, the part bed moves down by one layer thickness and powder is again spread by the re-coater. The sintered material forms the volume of the part while the un-sintered powder remains in its place acting as a support and is cleaned away once the build is complete. This process is repeated and prototype gets created.

The usual goals in SLS, or in any other RP method, during part fabrication are: (i) High quality surface finish (characterized by the minimization of surface roughness Ra), and (ii) Reduction of total build time T. Better surface finish can be achieved by deposition of thinner slices, but this is likely to increase the build time. Thus, there is usually a conflict between two simultaneously considered goals of achieving better surface quality and reduction in the build time. Both the objectives, Ra and T, depend on the build orientation (defined later) and the goal is to find orientations which is/are optimal.

In past, several studies have been carried out in order to identify optimal orientations by considering different objectives. Development of expert systems based on user experience was proposed in [5]. Preferential treatment of objectives categorized as primary (surface roughness) and secondary (build time) was attempted in [3]. Genetic algorithms were used to minimize a weighted sum of surface roughness and build time in context to different RP applications [17, 2, 1]. A bi-objective approach simultaneously considering build time and surface accuracy was proposed in [12, 13, 14, 15]. A complete recollection of past work is beyond the scope of interest in this paper, but an important fact to realize is that despite such attempts, a systematic application of nature inspired heuristics to carry out multi-objective optimization followed by decision-making and knowledge discovery through post-optimal analysis is still missing, which is the focus of this paper.

Once the trade-off front (and corresponding build orien-

tations) are found, the final step is the selection of an orientation for fabrication. To aid this step we have proposed three decision making schemes. Further, the importance of post optimal analysis of the solutions to unfold problem information is also demonstrated through case studies. The entire procedure is automated by developing a package called *Multi-objective Rapid Prototyping Engine* ($MORPE$). The software tool is developed for SLS system and is easily modifiable for other RP techniques. $MORPE$ incorporates two multi-objective evolutionary algorithms NSGA-II and MOPSO, statistical performance measures like attainment surface estimator and hypervolume calculator, 'Local Search' procedure to improve the solutions obtained from MOEAs, and 'Decision Making' schemes to facilitate the designer to select an optimum fabrication orientation. [1]

The rest of the paper is structured as follows. In section 2 the multi-objective problem formulation is provided. Section 3 briefly introduces the multi-objective evolutionary optimizers (NSGA-II and MOPSO) and statistically comparable performance measures adopted in this study. In section 5 several solid models are considered for bi-objective optimization to investigate and validate the working of $MORPE$. Results and discussions on the experiments are presented in section 6. This section also provides insight into the decision making and innovative design principles are deciphered via. post optimal analysis. Finally, in section 7 major findings of this study are summarized.

2. MULTI-OBJECTIVE PROBLEM

In current study, the objectives of interest are average surface roughness Ra and total build time T, both of which depend on the build orientation ϕ. The, bi-objective optimization problem considering Ra and T is formulated as:

Minimize $f_1 = Ra(\phi)$

Minimize $f_2 = T(\phi)$

with: $\phi = \{\theta_x, \theta_y\}$

subject to:

$0 \leq \theta_x \leq 180$

$0 \leq \theta_y \leq 180$

The decision variables θ_x and θ_y represent the rotations of solid model about X and Y axes, respectively, from an initial configuration about a chosen reference XYZ Cartesian coordinate system. For complete details on rotations, reader is referred to [12]. The optimization problem has two minimization type objectives which depend upon two decision variables. The decision variables are bounded in a range and there are no other constraints. Next, we briefly discuss the computation of Ra and T which is borrowed from [16].

In a CAD model an object is represented by triangular facets. So the first step is to compute the roughness of a single facet. Following equations are used for calculating the roughness depending upon whether the facet is 'up' or 'down' facing:

$$Ra_{up} = -2.04067 + .22\alpha + 0.06722t - 0.001368\alpha^2 \quad (1)$$

$$Ra_{down} = 185 - 9.52P - 0.834\alpha - 0.157t + 0.15P^2 - 0.00099\alpha^2 + 0.0058\alpha t \quad (2)$$

Here, angle $\alpha = 90^\circ - \theta$, where θ is the angle between vertical direction and facet normal as shown in Figure 1, 't' is the slice thickness (taken as 0.15 mm) and 'P' is the laser power (taken to be 60 W). Once, roughness values are computed for all the facets the Average Surface Roughness (Ra) of the entire part can be calculated as:

$$Ra_{av} = \frac{\sum Ra_i A_i}{\sum A_i} \quad (3)$$

where Ra_i and A_i are the surface roughness and area of the i^{th} facet. At build angle α=90° or α=0° the roughness value from these equations differ. At this angle roughness is computed by taking the average of the two models. The variation of roughness values for 'up' or 'down' facing facets is shown in Figure 2.

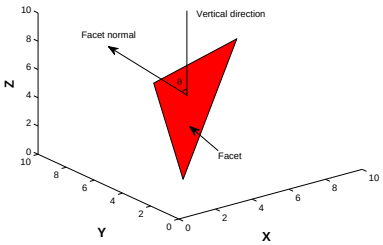

Figure 1: Build angle computation for a triangular facet.

The majority the build time in SLS occurs during recoating of the powder, in which case T is proportional to the number of layers. Since the layers are of constant thickness, T becomes proportional to object height in the build direction. Therefore, by minimizing the height of the part in the direction of deposition, build time can be minimized. If Z-axis denotes the build direction then the build time estimate is given by object height as:

$$T = (Z_{max} - Z_{min}) \quad (4)$$

3. PROPOSED APPROACH

The overall procedure is carried out by $MORPE$ which comprises of following modules: a) Multi-objective optimizers-NSGA-II and MOPSO b) Performance comparison tools– Hypervolume Indicator and Attainment Surface Approximator c) Local Search Tool d) Decision Making Kit. Figure 3 portrays the working of MORPE.

Although there exist several multi-objective evolutionary algorithms (MOEAs) in literature, popularly used genetic algorithm based (NSGA-II) and particle swarm based (MOPSO) optimizers have been utilized in this study. NSGA-II is an Elitist Non-Dominated Sorting Genetic Algorithm and one of the most popularly used GA for multi-objective optimization. Several salient features like elite preservation and explicit diversity preserving mechanisms ensure its good convergence and diversity. More details on NSGA-II can be

[1]This tool is made freely downloadable from xxxxxand should serve as useful resource for entire RP community.

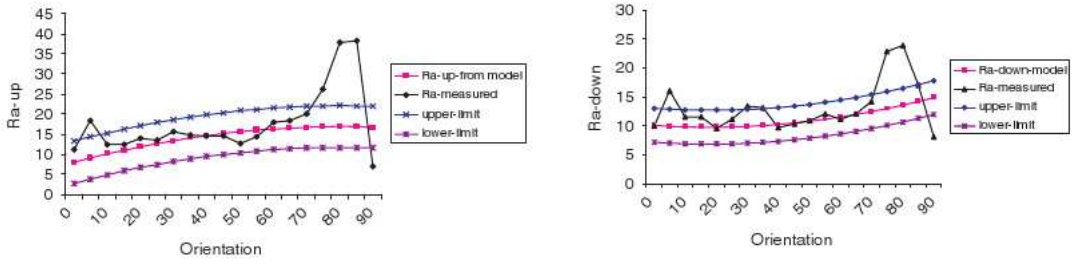

(a) (b)

Figure 2: (a) Variation of Ra-up with respect to build angle. (b) Variation of Ra-down with respect to build angle. The laser power(P) is 60 W and thickness(t) is 0.15 mm, also taken in this study.

found in [4]. Recently, Multi-objective Particle Swarm Optimizers have also gained popularity. A recently proposed MOPSO in [11, 10] has been adopted in this study. The MOPSO uses *NWtd.* and *Dom.* methods for personal best and global best selections. Clustering method is used for archiving purposes. For more details on MOPSO reader is referred to [11, 9]. By employing two evolutionary optimizers we are able to approximate the Pareto-front with better accuracy.

Due to stochastic nature of evolutionary approaches, it is difficult to conclude anything from just one simulation. To eliminate the random effects and gather results of statistical significance, we perform multiple (11) runs of the evolutionary algorithm corresponding to different initial populations. Two performance measures commonly used in EA literature have been employed in this paper, and described as follows:

Attainment Surfaces: Multiple non-dominated sets from multiple runs are used to deduce an approximation of best non-dominated set, commonly known as 1^{st} attainment surface. The computation of attainment surfaces is done by using attainment surface package described in [6].

Hypervolume indicator: Hypervolume is a measurement which takes into account the diversity as well as the convergence of the solutions [18]. Hypervolume represents the sum of the areas enclosed within the hypercubes formed by the points on the non-dominated front and a chosen reference point. For minimization type problems a higher value of hypervolume is desired, as it indicates better spread and convergence of solutions.

As a usual practice in MO applications, we employ mutation driven hill-climbing strategy and conduct *local search* to refine the best non-dominated set obtained from the evolutionary optimizers. However, for majority of experiments in this paper, little or no improvement was found after the local search – indicating the closeness of obtained solutions to Pareto solutions. The local search was carried out based on achievement scalarizing function [9] but due to space limitations we exclude any further details.

4. DECISION MAKING

When a set of trade-off solutions is obtained from a multi-objective optimization exercise, a decision point needs to be chosen to proceed further. This is often a non-trivial task for an operator and guidelines are desired. To address this task, we introduce three decision making techniques, namely– *'Aspiration Point Method'*, *'Marginal Utility Method'* and *'L_2 Metric Method'* [8]. The first method requires an 'aspiration point', described later, as an input from the user. However, remaining two methods do not require any user input. These methods are described as follows:

Aspiration Method: This method assumes that the designer has some pre-decided preference (or aspiration) for an operating point with which he/she is likely to settle. The goal is to find a solution which is better than the aspiration of the designer, thereby calling it an aspiration point method. To carry out the search we allocate this aspiration point as the reference for ASF scheme [8], and evaluate ASF for all points on the Pareto-optimal front. The Pareto-optimal solution which corresponds to lowest ASF value, with respect to the reference point, is selected.

In this study we have considered following three aspiration points:

$Asp_1 = (\frac{Ra_{min}+Ra_{max}}{2}, \frac{T_{min}+T_{max}}{2})$, $Asp_2 = (\frac{Ra_{min}+Ra_{max}}{2}, T_{max})$, $Asp_3 = (Ra_{max}, \frac{T_{min}+T_{max}}{2})$

Asp_1, for example, implies that user is willing to accept an available point in proximity of (but better than) the mean of best and worst obtained (Ra, T) values. The corresponding decision choices obtained on the Pareto-front are indicated as P_1, P_2 and P_3.

Marginal Utility Method: This approach does not require any prior information from the user and searches for a Pareto-optimal solution which shows least affinity towards any of its neighbors in the objective space. To compute this affinity, consider three non-dominated points P_1, P_0 and P_2, s.t. $(Ra_1 \leq Ra_0 \leq Ra_2)$ and $(T_1 \geq T_0 \geq T_2)$ and we are interested in evaluating the affinity at the middle point P_0. P_1

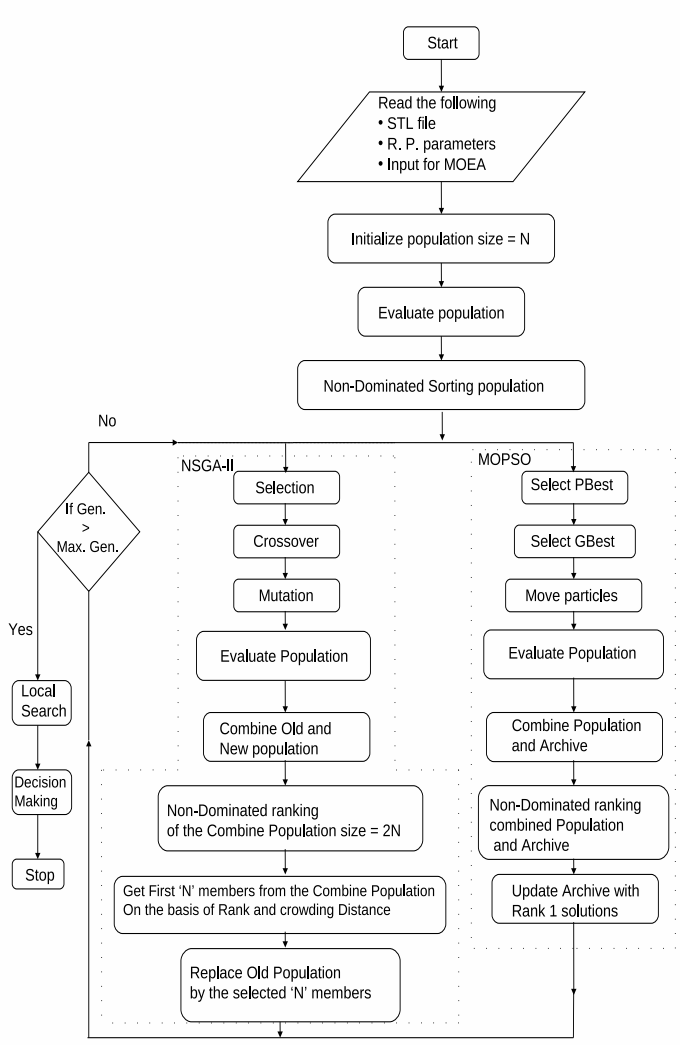

Figure 3: Flowchart suggesting the working of developed engine

and P_2 lie in the neighborhood of P_0 and are selected as follows: consider k points, $P_{0,m}$ m = 1 to k, nearest to P_0, with $Ra_{0,m} \leq Ra_0$. Then centroid of all $P_{0,m}$s is computed and a point out of $P_{0,m}$s, which is closest to the centroid, is selected as P_1. For selecting P_2, same exercise is repeated, but this time considering points s.t. $Ra_{0,m}$s are greater than Ra_0.

Once P_1 and P_2 are computed for P_0, *affinity function* (AF), is calculated as :

AF_{P_0}=max(W1,W2); W1= $\frac{Ra_{P_0}-Ra_{P_1}}{T_{P_1}-T_{P_0}}$ and W2= $\frac{Ra_{P_2}-Ra_{P_0}}{T_{P_0}-T_{P_2}}$.

For each point in the non-dominated set, except for k extreme points at both ends, AF is computed and the solution with minimum AF is assigned as decision choice. This solution is argued to posses *least affinity to move away from.* In this study value of k is taken equal to 6. The value of k decides the resolution of the proximity in which we are interested to compute the affinity function. Decision point found by this method is usually a *'knee point'. 'Knee points'* are of great practical importance as they denote a coordinate on Pareto-front where increase (decrease) in one objective is very large compared to decrease (or increase) in other objective.

L_2-metric: This approach also does not require any information from the user. Firstly, each objective is normalized in [0.0, 1.0]. Then an *'ideal point'* is constructed, which is origin in case of normalized space, and taken as the reference point. Euclidean distance (L_2) of each point in non-dominated set is calculated from the reference point and the solution with smallest euclidean distance is finally selected.

5. EXPERIMENTS

A series of simulations are performed on various solid models (ranging from simple geometries to complex ones) to find the optimal build orientations and trade-off fronts of Ra and T. A total of 9 solid models are considered in this study: Bipyramid, Pyramid, Prism, Pentagon-Bar, Disc, Cylinder, Diamond, Cuboid and Fin. These objects serve as a good representative set for different geometrical features.

Both NSGA-II and MOPSO are applied and performance of these optimizers are compared based on hypervolume curves and attainment surfaces. A population size of 40 and maximum number of generations 80 are chosen for both the optimizers. For NSGA-II crossover probability is taken as 0.9 and mutation probability as 0.5, other parameters are set as default. For MOPSO a t_f of 0.25 is used [11]. For each solid model both the optimizers are executed for 11 runs. Results from multiple runs from both the optimizers are combined and global non-dominated set is found. On each member of this global non-dominated set local search is applied. Negligible or no improvement is found in most cases, indicating the closeness of solutions to the actual Pareto-optimal set.

The $1^{st}(0\%)$ attainment surface is computed for both the optimizers, which serves as the best approximation of Pareto-front. Study of shapes and spread of Pareto-fronts along with the orientations corresponding to extreme solutions are also done. Based on the results the solid models have been categorized into two groups and general guidelines for optimal orientations are drawn. Important task of decision making is also carried on a sample object and usefulness of decision schemes is also highlighted.

6. RESULTS AND DISCUSSIONS

Estimation of minimum T orientation for SLS can be done by aligning the shortest object dimension along the build direction. But, minimum Ra orientation is non-intuitive as Ra computation is based on the weighted average of 'up' and 'down' facing surfaces. Moreover, at orientations in which majority of the model's surface area has a build angle α in proximity of 90° or 0° , Ra is expected to shown an erratic behavior.

We performed the simulations and categorized the objects into two groups based on commonalities amongst optimal solutions: (a) Solid models for which a distributed set of trade-off solutions is obtained, and (b) Solid models for which there is only a small variation in Ra or T, or practically no trade-off front is found. For group (a) objects, objectives are evidently conflicting leading to a reasonable range of trade-off solutions, whereas for group (b) the objectives are

almost non-conflicting leading to solutions within a small range. The two groups are discussed next:

Group (a): For Bipyramid, Figures 4(a) and 4(b) show average hypervolume curves and 1^{st} attainment surface for NSGA-II and MOPSO, respectively. L_2-metric the decision choice is also marked and occurs to be 'knee' point. NSGA-II hypervolume attains a steady value after 30 generations and stays above the hypervolume curve of MOPSO. Although, in initial few generation MOPSO shows a faster rise in hypervolume but fails to match NSGA-II performance. Based on the attainment surface curves as well, performance of NSGA-II is better than MOPSO (indicated by better spread and convergence of the trade-off front). However, both NSGA-II and MOPSO have similar trade-off front providing a better estimate on the location of Pareto-front. Such trends were also observed for other solid models but due to space limitations we only show these curves for Bipyramid. NSGA-II showed better performance over MOPSO for other solid models as well, detailed graphs have not been included.

'Reference Point Method' and 'Marginal Utility' schemes are shown in Figures 5(a) and 5(b), respectively. For 'Reference Point Method' three solutions corresponding to three reference points are obtained. The 'Marginal Utility Method' finds a 'knee' solution. Decision choices obtained for three methods suggests that 'L_2-metric method' and 'Marginal Utility' method favor to discover a knee solution on the trade-off front and do not depend upon any user information. 'Aspiration Method' is more flexible in finding solutions which resemble user's preference. However, the solutions found by'Aspiration Method', corresponding to a chosen reference point, depends on the shape and spread of the Pareto-front. The three decision schemes showed similar behavior on trade-off fronts of other solids and we do not present any further plots.

The min. T orientation, Figure 6(a), is achieved such that Bipyramid almost lies flat on one of the faces and minimum height occurs along Z-axis (build direction). Bipyramid has equal areas, hence the orientation which minimizes the surface roughness will be one in which the sum of all surface roughnesses is minimized. From the Ra model described earlier (Figure 2), roughness for a face is minimum when α is close to zero whether 'up' or 'down' facing. With the geometry of Bipyramid it is impossible to achieve an orientation where all (or a majority) of surfaces have 0° build angle. In such situation a best compromise which minimizes the sum of surface roughnesses is achieved when Bipyramid is slightly tilted from the vertical with majority of surfaces 'up' facing and one face close to being vertical, as shown in Figure 6(b). (Based on models the roughness is small for 'up' facing surfaces compared to 'down' facing for small values of α, which explains the fact that majority of surfaces are 'up' facing). The L_2-metric orientation shown in Figure 6(c) lies in between two extreme orientations.

The arguments provided above also serve to explain optimal orientations for remaining objects in this group. For Prism, in the min. T orientation, Figure 6(f), the object lies flat on the larger face. In min. Ra orientation, Figure 6(g), 4 out of 5 surfaces are either 'up' facing or vertical and Prism assumes an inclined orientation with respect to the horizontal such that one of the larger faces is vertical. For Pentagon Bar min. T orientation, Figure 6(h), occurs with the object lying flat on one its faces thereby leading to min-

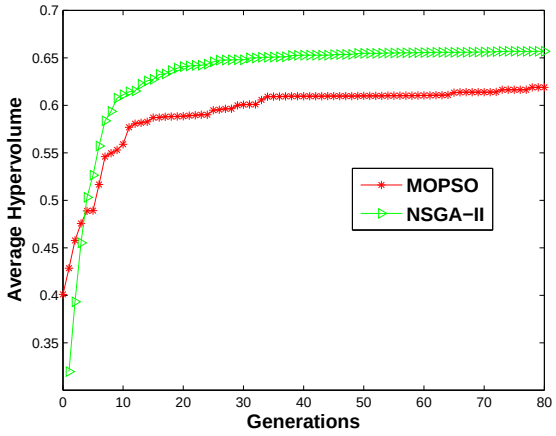

(a)

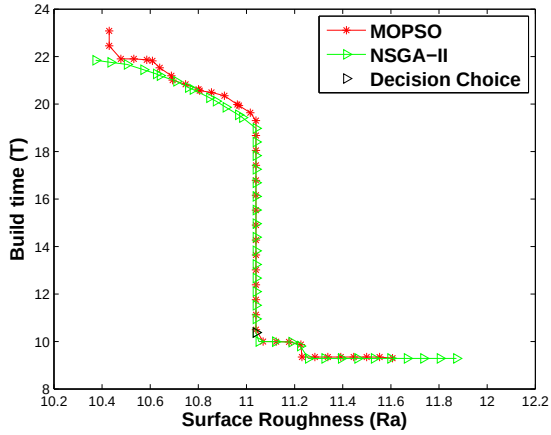

(b)

Figure 4: (a) NSGA-II and MOPSO hypervolume curves for Bipyramid with reference point (11.5, 11.0). (b) 1^{st} Attainment Surfaces for NSGA-II and MOPSO and L_2-metric 'Decision Choice' for Bipyramid.

imum height along Z-axis. In min. Ra orientation, Figure 6(h), all the large faces of the bar are vertical causing the build angle α=0°. For Disc min. T orientation, Figure 6(j), occurs with Disc lying horizontally flat, allowing minimum dimension (disc height) along Z-axis. The min. Ra orientation, 6(g), occurs with flat surfaces of disc vertical. In vertical position, (α=0°), flat surfaces have least roughness values. Majority area of flat surfaces (compared to curved surface), assigns more weight to lower roughness and overall Ra is minimized.

To validate our line of arguments, Cylinder is shown next. The length of the Cylinder is chosen to be larger than its diameter (unlike Disc). The minimum T orientation occurs with Cylinder lying horizontal and flat faces vertical, Figure 6(l). In minimum Ra orientation, Figure 6(m), Cylinder

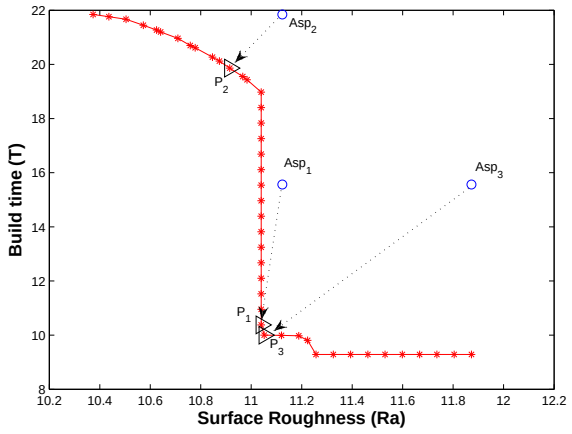

(a)

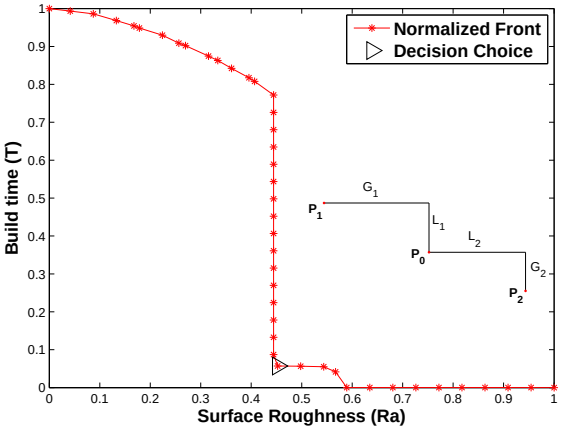

(b)

Figure 5: (a) Reference Point method for Bipyramid. (b) Marginal Utility method for Bipyramid.

stands tall vertically on one of the flat surfaces. This configuration is justified because larger curved surface area has lower surface roughness in vertical position with α=0°, and as Ra is weighted with surface area, min. Ra is achieved in this orientation. Next object considered is Diamond. The minimum T orientation, Figure 6(n), is self explanatory. The min. Ra orientation, Figure 6(o), occurs with axis of Diamond titled with respect to vertical and flat top facing 'down' and major portion of the curved surface area facing 'up'. For Diamond the curved surface area is larger than the flat top area, and from previous discussions we already have noted that 'down' faces lead to higher roughness compared to 'up' faces (up to certain α values). Hence in min. Ra majority of Diamond's area faces 'up'.

Group (b): This group consists of solid objects for which optimal solutions are found in a small span of distribution. Solid models in this group are Cuboid, Pie and Fin. For all these objects it is found that the spread of solutions in first or second objective is practically negligible. For Cuboid, min. T solution is with (θ_x,θ_y)=(90.0°, 90.0°) and (Ra, T)= (10.52, 10.0), and min. Ra solution is with (θ_x,θ_y)= (0.0°, 89.98°), (Ra, T)= (9.05, 10.0). In 3-D these two orientations are flat (89.98° is same as 90.0° for any practical purpose). Due to space limitation only Min. T solution is shown, Figure 6(p). The estimate of T for both these orientations is same but there is slight variation in Ra values. The variations can be explained based on numerical errors and discontinuity in Ra occurring due to vertical flat surfaces (α = 90.0°,90.0°). The flat orientation is justified as min. T solution as shortest height is along Z-axis. This orientation also has 4 surfaces (majority of the surface area) almost vertical ($\alpha = 0°$), thus leading to minimum Ra.

Next, for the Pie shape flat orientation, Figure 6(q), is the optimal orientation. Min. T in this orientation is self-evident. In this orientation the side-strip has $\alpha = 0°$. Although the side-strip is not the majority area, and the majority area faces lie horizontal with $\alpha = 90°$, still this orientation leads to min. Ra. To understand this behavior other orientations are shown in which majority surface areas have $\alpha = 0°$, Figures 6(r) and 6(s). It is found that T and Ra values are larger for these orientations. This can be explained based on the fact that though in these two orientations, the flat vertical surfaces have $\alpha = 0°$, but the remaining area on the strip has large α values which increases Ra. (It is important to note that in Figure 6(q), the roughness for top and bottom surfaces is not maximum rather an average of roughness at $\alpha = 0°$ and $\alpha = 90°$, and hence Ra is not large). For Fin as our last example, Figure 6(t) shows that the majority of surface (containing hollow feature and protruding plates) has $\alpha = 0°$ (thereby minimizing Ra) and the minimum vertical thickness minimizes T.

For all the solid models that we have considered the optimal extreme orientations have been explained well in consonance with the objective function models. Thus, our procedure is validated. Importantly, similar trade-off fronts obtained by two popular optimizers builds our confidence in the proposed approach. Based on studies conducted here, an insight into the nature of optimal orientations is also obtained. Minimum T orientation for objects is straightforward to guess and occurs when shortest dimension occurs along Z-axis. Certain guidelines for min. Ra orientations can be derived as follows. For objects with flat surfaces only, a min. Ra orientation occurs when the faces with the majority area are (or close to) vertical. When curved or oblique surfaces appear on the object then an orientation in which majority area is vertical is often non-optimal. In such cases, the build angle for curved or oblique faces should be reduced and often one may find min. Ra orientation coinciding with min. T orientation. The scope of these rules can be made broader by conducting such studies on several objects to derive general principles which may help the designer to guess an optimal orientation a-priori. Before conducting this study, to get such an insight would not have been possible.

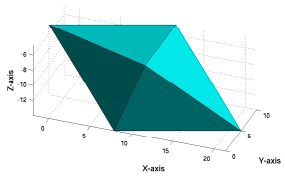

(a) Min. T orientation (θ_x,θ_y)= (0.0°, 111.81°), (Ra, T)= (11.87, 9.29)

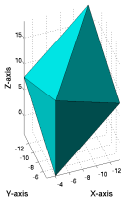

(b) Min. Ra orientation (θ_x,θ_y)= (158.2°, 159.63°), (Ra, T)= (10.37, 21.76)

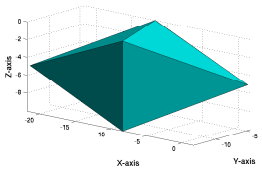

(c) L_2-metric Decision Choice orientation for (θ_x,θ_y)= (159.94°, 90.01°), (Ra, T)= (11.04, 10.00)

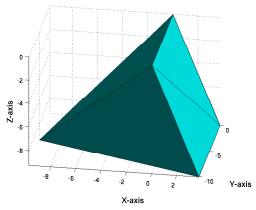

(d) Min. T orientation (θ_x,θ_y)= (180.0°, 68.19°), (Ra, T)= (11.77, 9.29)

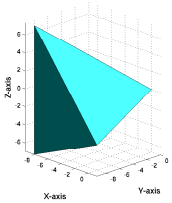

(e) Min. Ra orientation (θ_x,θ_y)= (158.2°, 159.64°), (Ra, T)= (8.72, 14.36)

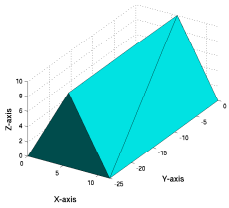

(f) Min. T orientation (θ_x,θ_y)= (90.0°, 0.0°), (Ra, T)= (12.29, 10.02)

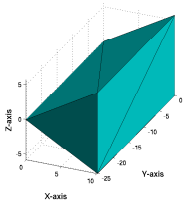

(g) Min. Ra orientation (θ_x,θ_y)= (89.99°, 29.99°), (Ra, T)= (8.71, 11.57)

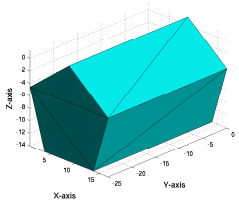

(h) Min. T orientation (θ_x,θ_y)= (90.0°, 81.45°), (Ra, T)= (11.89, 15.38)

,

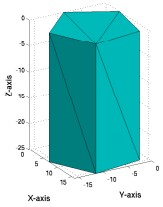

(i) Min. Ra orientation (θ_x,θ_y)= (179.99°, 0.02°), (Ra, T)= (9.15, 25.0)

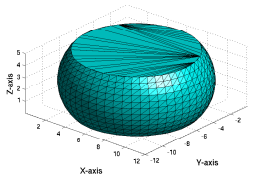

(j) Min. T orientation (θ_x,θ_y)= (90.0°, 0.0°), (Ra, T)= (12.13, 5.0)

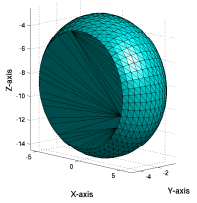

(k) Min. Ra orientation (θ_x,θ_y)= (180.0°, 43.33°), (Ra, T)= (10.85, 12.05)

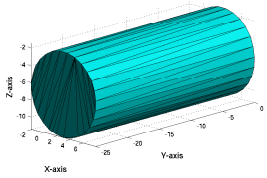

(l) Min. T orientation (θ_x,θ_y)= (90.0°, 110.09°), (Ra, T)= (10.73, 9.99)

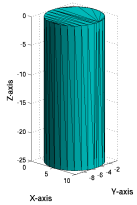

(m) Min. Ra orientation (θ_x,θ_y)= (179.98°, 0.0°), (Ra, T)= (9.13, 25.0)

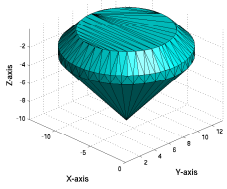

(n) Min. T orientation (θ_x,θ_y)= (0.0°, 180.0°), (Ra, T)= (12.04, 10.0)

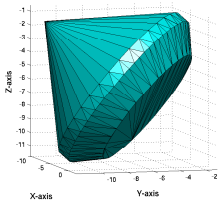

(o) Min. Ra orientation (θ_x,θ_y)= (138.3°, 145.24°), (Ra, T)= (11.07, 11.26)

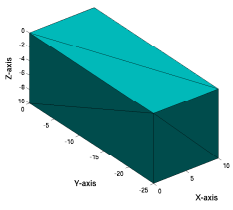

(p) Optimal orientation (θ_x,θ_y)= (90.0°, 90.0°), (Ra, T)= (10.52, 10.0)

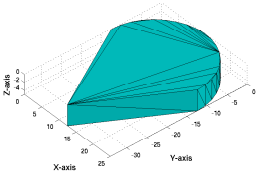

(q) Optimal orientation (θ_x,θ_y)= (180.0°, 0.0°), (Ra, T)= (10.43, 5.0)

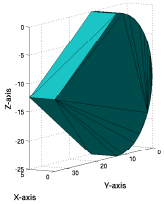

(r) Orientation with (θ_x,θ_y)= (0°, 90°), (Ra, T)= (11.16, 25.0)

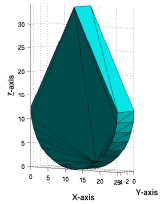

(s) Orientation with (θ_x,θ_y)= (90°, 0°), (Ra, T)= (11.85, 34.1)

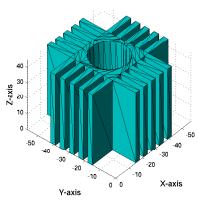

(t) Optimal orientation (θ_x,θ_y)= (180.0°, 180.0°), (Ra, T)= (9.27, 45.0)

Figure 6: (a)-(c) Byramid. (d)-(e) Pyramid. (f)-(g) Prism. (h)-(i) Pentagon-Bar. (j)-(k) Disc. (l)-(m) Cylinder. (n)-(o) Diamond. (p) Cuboid. (q)-(r) Pie. (s) Fin.

7. CONCLUSIONS

This paper presents a novel attempt and systematic approach to address the tasks of finding optimal build orientations in SLS process, approximating true (or close to) Pareto-optimal solutions, and addressing the issue of decision-making. The entire procedure is integrated and leads to the development of $MORPE$ – Multi-objective Rapid Prototyping Engine. Two popular optimizers, NSGA-II and MOPSO, are employed to discover trade-off fronts. Overall NSGA-II outperforms MOPSO, but similarities in convergence and spread patterns of trade-off fronts indicate the closeness of obtained solutions to the Pareto-front. Local search employed to fine tune the obtained solutions showed negligible improvement, assuring that the solutions found by the optimizers are pretty good estimate of Pareto-solutions. Several sample objects considered for experimentation demonstrated the working of optimizers and decision making schemes. 'Reference Point Method' discovers a solution which depends on the user's preference and the shape of the Pareto-front. 'Marginal Utility Method' and '$L_2 - metric$' methods have a tendency to discover a 'knee' point.

Based on the nature of the optimal solutions and careful analysis, objects could be categorized into two groups. For the first group a reasonable spread amongst the trade-off solutions was found. The second group objects were found to have a single optimal orientation which minimizes both Ra and T. A closer analysis of the obtained solutions in consideration with their geometric features and Ra model helps in revealing common characteristics amongst the optimal orientations. Such a discovery is regarded useful from a practical view-point and may aid a designer in guessing optimal orientations for a solid object based on its geometry.

8. REFERENCES

[1] Daekeon Ahn, Hochan Kim, and Seokhee Lee. Fabrication direction optimization to minimize post-machining in layered manufacturing. *International Journal of Machine Tools and Manufacture*, 47(3-4):593 – 606, 2007.

[2] Hong-Seok Byun and Kwan H. Lee. Determination of the optimal build direction in layered manufacturing using a genetic algorithm. *Internation Journal of Production Research*, 43(13):2709–2724, 2005.

[3] W. Cheng, J. Y. H. Fuh, , A. Y. C. Nee, Y. S. Wong, H. T. Loh, and T. Miyazawa. Multi-objective optimization of part-building orientation in stereolithography. *Rapid Prototyping Journal*, 1:22–33, 1995.

[4] K. Deb. *Multi-objective Optimization Using Evolutionary Algorithms*. John Wiley and Sons, Dordrecht, 2001.

[5] D. Frank and G. Fadel. Expert system-based selection of the preferred direction of build for rapid prototyping processes. *Journal of Intelligent Manufacturing*, (6):339–345, 1995.

[6] J. Knowles. A summary-attainment-surface plotting method for visualizing the performance of stochastic multiobjective optimizers. In *IEEE Intelligent Systems Design and Applications (ISDA V)*, pages 552–557, 2005.

[7] J.P. Kruth, M.C. Leu, and T. Nakagawa. Progress in additive manufacturing and rapid prototyping. *Annals of CIRP*, 47(2), 1998.

[8] K. Miettinen. *Nonlinear Multiobjective Optimization*. Kluwer, Boston, 1999.

[9] N. Padhye. Comparision of archiving methods in mopso: Empirical study. In *GECCO '09: Proceedings of the 2009 GECCO conference companion on Genetic and evolutionary computation*.

[10] N. Padhye. Topology optimization of compliant mechanism using multi-objective particle swarm optimization. In *GECCO '08: Proceedings of the 2009 GECCO conference companion on Genetic and evolutionary computation*, pages 1831–1834.

[11] N. Padhye, J. Juergen, and S. Mostaghim. Empirical comparison of mopso methods - guide selection and diversity preservation -. In *Proceedings of Congress on Evolutionary Computation (CEC), in press*. IEEE, 2009.

[12] N. Padhye and S. Kalia. Rapid prototyping using evolutionary algorithms: Part 1. In *GECCO '09: Proceedings of the 2009 GECCO conference companion on Genetic and evolutionary computation*, 2009.

[13] N. Padhye and S. Kalia. Rapid prototyping using evolutionary algorithms: Part 2. In *GECCO '09: Proceedings of the 2009 GECCO conference companion on Genetic and evolutionary computation*, pages 2737–2740, 2009.

[14] P. M. Pandey, K. Thrimurthulu, and N. V. Reddy. Optimal part deposition orientation in fdm by using a multicriteria. *International Journal of Production Research*, 42 (19):4069–4089, 2004.

[15] P.M. Pandey, N. Venkata Reddy, and S.G. Dhande. Part deposition orientation studies in layered manufacturing. *Journal of Materials Processing Technology*, 185:125–131, 2007.

[16] S.K. Singhal, Prashant K. Jain, Pulak M. Pandey, and A.K. Nagpal. Optimum part deposition orientation for multiple objectives in sl and sls prototyping. *International Journal of Production Research*, 47 (22):6375–6396, 2009.

[17] K. Thrimurtullu, P.M. Pandey, and N. V. Reddy. Optimum part deposition orientation in fused deposition modeling. *International Journal of Machine Tools and Manufacture*, 4(6):585–594, 2004.

[18] E. Zitzler. *Evolutionary Algorithms for Multiobjective Optimization: Methods and Applications*. PhD thesis, ETH Zurich, Switzerland, 1999.